Journal of Earth Science, *Vol. 36*, *No. 2*, *p. 627–643*, *April 2025* *ISSN 1674-487X*
Printed in China
https://doi.org/10.1007/s12583-022-1804-0

Development Conditions and Factors Controlling the Formation of the Permian Pingdiquan Source Rocks in the Wucaiwan Sag, Junggar Basin, China: A Comprehensively Elemental, Biomarker and Isotopic Perspective

Jinqi Qiao[1, 2], **Hao Li**[3], **Qingyong Luo**[*1, 2], **Luofu Liu**[1, 2], **Dandan Wang**[1, 2], **Xiaoqing Shang**[4], **Fei Xiao**[5], **Tong Zhang**[6]

1. *State Key Laboratory of Petroleum Resources and Engineering*, *China University of Petroleum* (*Beijing*), *Beijing* 102249, *China*
2. *College of Geosciences*, *China University of Petroleum* (*Beijing*), *Beijing* 102249, *China*
3. *Wuxi Institute of Petroleum Geology of SINOPEC*, *Wuxi* 214126, *China*
4. *School of Earth Sciences and Engineering*, *Xi' an Shiyou University*, *Xi' an* 710065, *China*
5. *Shenyang Center of China Geological Survey*/*Northeast Geological S & T Innovation Center of China Geological Survey*, *Shenyang* 110034, *China*
6. *Xinjiang Oilfield Company*, *Petrochina*, *Karamay* 834000, *China*

Jinqi Qiao: https://orcid.org/0000-0001-6240-6389; Qingyong Luo: https://orcid.org/0000-0002-1176-5709

ABSTRACT: This paper is a synthetic use of carbon isotope composition, Rock-Eval data, organic petrology, element composition of kerogen, major and trace elements, and biomarker characteristic of the Permian Pingdiquan (P_2p) source rocks in the Wucaiwan sag, Junggar Basin, China as proxies (1) for evaluations of hydrocarbon potential, organic matter (OM) composition and thermal maturity of the OM in the source rocks, (2) for reconstruction of paleodepositional environment, and (3) for analysis of controlling factor of organic carbon accumulation. The P_2p Formation developed good-excellent source rocks with thermal maturity of OM ranging from low-mature to mature stages. The OM was mainly composed of C_3 terrestrial higher plants and aquatic organisms including aerobic bacteria, green sulfur bacteria, saltwater and fresh algae, Sphagnum moss species, submerged macrophytes, Nymphaea, and aquatic pollen taxa. The proportion of terrestrial higher plants decreased and that of aquatic organisms increased from margin to center of the sag. The benthic water within reducing environment and brackish-water column were superposed by periodic/occasional fresh-water influx (e.g., rainfall and river drain), which led to fresh-water conditions and well oxygenating in the water column during overturn process. The whole study area developed lacustrine source rocks without seawater intrusion. During periodic/occasional fresh-water influx periods with plenty of terrestrial plant inputs, the paleoredox conditions of the sag were relatively oxic in the shallow fresh-water which experienced strong oxidation and decomposition of OM, therefore were not conducive for the OM preservation. However, the overall middle primary productivity made up for this deficiency, and was the main controlling factor on the organic carbon accumulation. A suitable supply from terrestrial inputs can promote biotic paleoproductivity, and a relatively high sedimentation rate can reduce oxidation and decomposition times of OM. On the contrary, during the intervals of the fresh-water influxes, relatively reducing conditions are a more important controlling factor on the OM accumulation in the case that the decrease of the terrestrial biotic source.

KEY WORDS: geochemistry, source rocks, paleodepositional environment, Pingdiquan Formation, Junggar Basin.

*Corresponding author: qingyong.luo@cup.edu.cn

Manuscript received April 7, 2022.
Manuscript accepted December 15, 2022.

0 INTRODUCTION

It is generally recognized that the enrichment and distribution of organic matter (OM), as well as the development and hydrocarbon (HC) potential of source rocks, are mainly controlled by primary paleoproductivity (organ-

Qiao Jinqi, Li Hao, Luo Qingyong, Liu Luofu, Wang Dandan, Shang Xiaoqing, Xiao Fei, Zhang Tong, 2025. Development Conditions and Factors Controlling the Formation of the Permian Pingdiquan Source Rocks in the Wucaiwan Sag, Junggar Basin, China: A Comprehensively Elemental, Biomarker and Isotopic Perspective. *Journal of Earth Science*, 36(2): 627–643. https://doi.org/10.1007/s12583-022-1804-0. http://en.earth-science.net

ic carbon fluxes) (Gallego-Torres et al., 2007; Caplan and Bustin, 1999) or paleoredox condition (Mort et al., 2007; Demaison and Moore, 1980). Besides, OM accumulation in each sedimentary setting was likely controlled by its unique factors which may respond to the synthetic effects of these two factors or maybe a single factor (Schoepfer et al., 2015; Rimmer, 2004).

The OM in the source rocks is mainly derived from the decomposition of terrestrial organic debris and aquatic organisms, and the matrix is mainly transported from eroded clastics in the continental provenances of the drainage area in forms of dissolved and particulate materials via chemical weathering of rocks. Biomarker and carbon isotopic composition of OM ($\delta^{13}C_{org}$) inherit information about OM source, sedimentary environment, thermal maturity of OM, and HC migration (Hunt, 1996; Peters and Moldowan, 1993). Besides, ratios of carbon (C) to nitrogen (N) determined from elemental analysis of OM can be used to analyze OM origins (Zhu et al., 2022; Meyers, 1994). However, each indicator is influenced by some factors, such as diagenesis, thermal maturity of OM and contaminantion, and has a specific scope of application in interpreting OM characteristics, paleodepositional environment and paleoclimate. Therefore, on the one hand, it is necessary to use multiple proxies to clarify one issue; on the other hand, coupling $\delta^{13}C_{org}$ values with each of C/N ratios and total organic carbon (TOC, wt.%) contents can be used to assess OM sources and controlling factors on OM accumulation (Lamb et al., 2006; Freeman et al., 1994, 1990; Hollander and McKenzie, 1991).

The Middle Permian Pingdiquan (P_2p) Formation deposited in the eastern Junngar Basin of China hosts large HC potential and shale-oil (Bai et al., 2017; Cao et al., 2017). However, the issues related to kerogen type, thermal maturity of OM, and paleosalinity are controversial in previous studies. Cao et al. (2017) argued that it was a typical saline lacustrine deposit and primarily consists of types II and III kerogens with the thermal maturity of OM ranging from early to late maturity stage. However, Bai et al. (2017) considered that the OM of the P_2p source rocks was dominated by Type II kerogen and is presently in the low mature-mature stage under fresh to brackish conditions. What's more, Carroll et al. (1992) proposed that the P_2p Formation was deposited in deltaic and lacustrine sedimentary environments, while Liang et al. (2014) argued that the late stage of the Middle Permian was a paralic epicontinental lacustrine environment which was influenced by seawater intrusion (Bai et al., 2017). Besides, the paleoproductivity in the eastern Junggar Basin during the Middle Permian period as well as the enrichment mechanism and controlling factor of the development of the P_2p source rocks have not been thoroughly analyzed.

This paper focuses on Rock-Eval data, organic petrology, elements compositions of kerogen and whole rock, biomarker characteristics and $\delta^{13}C_{org}$ composition of the P_2p source rocks in the Wucaiwan sag of the Junggar Basin. Firstly, the study aims to decipher the factors that control the development and paleodepositional conditions of the source rocks in the Wucaiwan sag. This may provide new clues to reconstructing its sedimentary environments and judging whether seawater intrusion occurred or not in the basin during the Permian. Secondly, the study of source rocks' biomarker characteristics can provide reliable bases for the following oil-source correlation and accumulation. Thirdly, the main factor controlling OM accumulation in terrestrial source rocks is unclear due to complex sedimentary environments and plenty of terrigenous inputs in sedimentary basins. Therefore, the effect of terrestrial inputs should be considered in the evaluation of organic carbon accumulation. This study provides a case study of a comprehensive approach to evaluating organic carbon accumulation in lacustrine environments by using multiple proxies.

1 GEOLOGIC SETTING

The Junggar Basin, a typical Late Palaeozoic, Mesozoic, and Cenozoic superimposed petroliferous basin, covers a 130 000 km^2 exploration area in NW China (Hou et al., 2021; Bai et al., 2017; Cao et al., 2017; Figure 1a). The basin was a marine and residual marine foreland basin, continental foreland basin, intracontinental oscillatory depression basin, and regeneration foreland basin during the Late Carboniferous – Early Permian, Middle – Late Permian, Mesozoic, and Cenozoic periods, respectively (Chen et al., 2015). The eastern Junggar Basin experienced multiphase tectonic cycles including the Hercynian, Indosinian, Yanshanian and Himalayan events after the Late Carboniferous (Wan et al., 2015). The Wucaiwan sag (around 949 km^2) is located in the eastern uplift belt of the basin and on the west of the Paleozoic sedimentary depression of the Kelameili Piedmont (Figure 1b). The sag's northern boundary connects to the Dinan high, its southeast boundary connects to the Shazhang fault-fold belt, and the sag connects to the Baijiahai high to the southwest. The sag began to form in the Late Carboniferous and the paleotopography was a northward dipping monocline, where the northern part was a steep-slope before the Permian.

The Wucaiwan sag developed Carboniferous, Permian, Triassic, Jurassic, Cretaceous, Paleogene, Neogene and Quaternary stratigraphy sets from bottom to up. The sag was developed in a faulted deep-water basin during the Permian period. According to lithologic association, sedimentary cycle and property of contact interface, the Permian strata can be divided into five formations: the Jingou (P_1j), Jiangjunmiao (P_2j), P_2p, Quanzijie (P_3q) and Wutonggou (P_3wt) Formation. Due to the influences of the paleoclimate and the foreland basin tectonic background of the Kelameili Piedmont, the P_1j and P_3q formations were undeveloped or had been weathered and denuded in the study area. The main sedimentary facies of the P_2p Formation in the study area were fan delta front, braided river delta front, shore-shallow lake, moderately deep lake, and deep lake facies. The P_2p Formation which is the most favorable source rocks in the study area developed gray and gray-black mudstone as well as

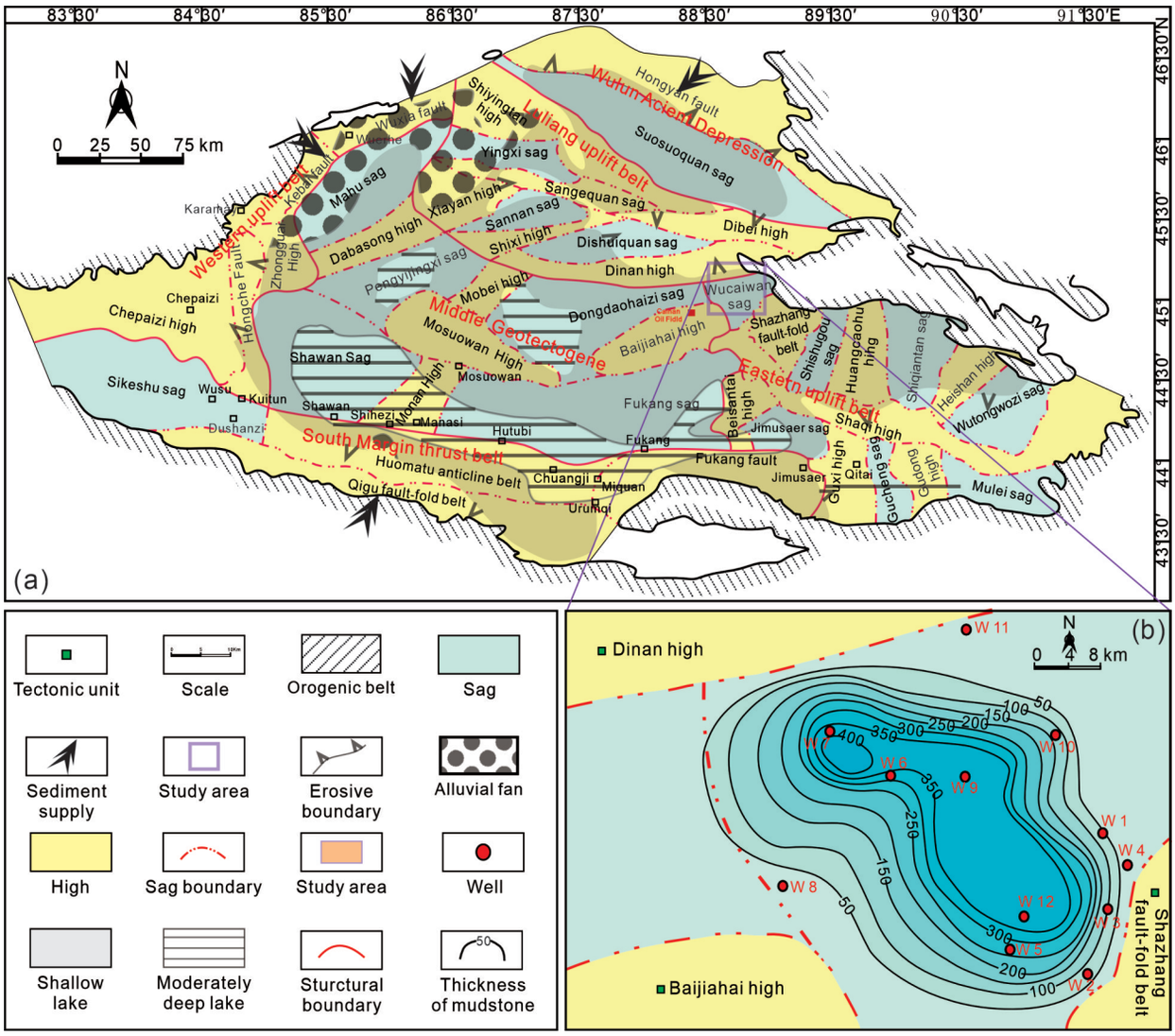

Figure 1. (a) The structure outline map of the Junggar Basin (after Qiao et al., 2020), lithofacies distribution during the Middle–Late Permian (Bian et al., 2010) and location of the studied area, as well as (b) distribution of the P_2p source rocks in the Wucaiwan sag.

black dolomitic mudstone with a thickness of 50–450 m (Figures 1c and 2).

2 SAMPLES AND ANALYTICAL METHODS

2.1 Samples and Data

In this study, all samples came from 11 wells. Amongst these wells, W1, W2, W3, W4, W5 and W12 wells are located in the southeast of the sag; Well W7 is located in the northwestern sag; wells W6 and W9 are located in the center of the sag; Well W8 is located in the southwest of the sag; wells W10 and W11 are located in the northeast of the sag (Figure 1c). As for the testing, 52 samples were used to measure TOC content; 48 samples were used for Rock-Eval pyrolysis; 58 samples' extractable OM (EOM) was precipitated and separated, and their saturated and aromatic HCs as well as NSO (N, sulfur (S) and oxygen (O)) compounds were separated and quantitatively analyzed and further used for biomarker analysis; 27 samples were used to identify maceral composition; major and trace element concentrations from 14 samples were measured; $\delta^{13}C_{org}$ and element composition of kerogen from 41 and 45 samples were tested, respectively. Before the measurements, fresh core samples were pulverized to a mesh size of < 200 using a tungsten carbide ball mill.

In this study, $\delta^{13}C_{org}$ and elemental composition were performed at the Chinese Academy of Science; biomarkers analysis, Rock-Eval pyrolysis and TOC content measurement were performed at the State Key Laboratory of Petroleum Resources and Engineering, China University of Petroleum (Beijing); and the R_o and organic petrology data were provided by the Cainan Oil Field.

2.2 Elemental Analysis

The measurement of elemental composition of kerogen (C, N, hydrogen (H), S, and O) was performed on a Vario EL cube element analyzer. At first, the powder samples were digested with hydrochloric acid (HCl) to remove carbonates and then hydrofluoric acid (HF) to remove silicates. After that, the residue was separated and

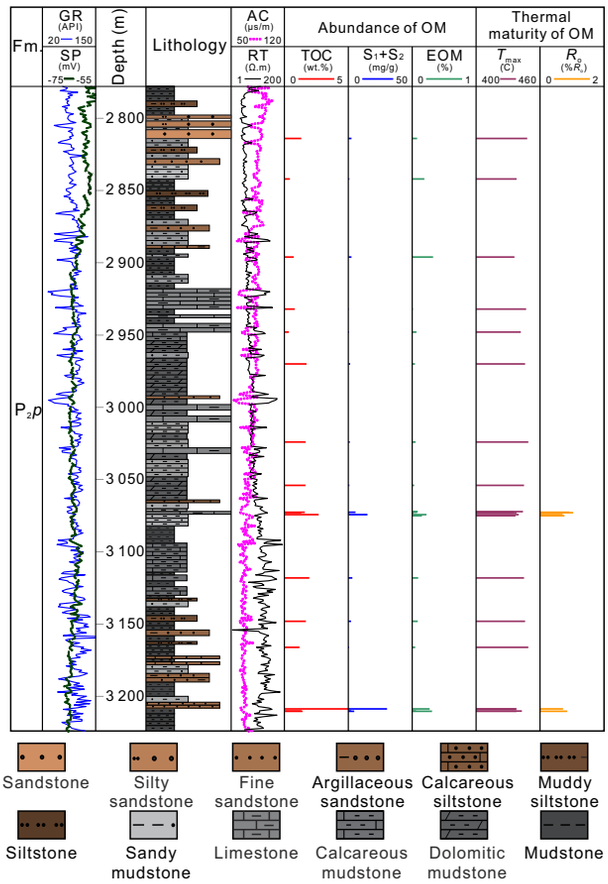

Figure 2. The stratigraphic column and geochemical parameters of Well W7 for the P_2p Formation in the Wucaiwan sag of the Junggar Basin, China.

extracted by heavy liquids and chloroform ($CHCl_3$) to obtain the soluble components. For the measurement, the first setup was filled with helium (He) and oxygen (O_2) at a specified temperature, then the weighted sample was placed into the analyzer. After pyrolysis, column chromatography, and thermal conductivity detection, the relative concentrations of each element in the kerogen were determined. Analytical accuracy and precision were ±10% and ±5%, respectively.

Major and trace elements were measured using an ARL Perform'X 4200 wavelength-dispersive X-ray fluorescence (WD-XRF) spectrometer and an ELAN DRC-e inductively coupled plasma mass spectrometer (ICP-MS), respectively. Detailed information related to the measurements was given by Qiao et al. (2022).

2.3 TOC Content and Rock-Eval Pyrolysis

TOC content was analyzed by combustion in a LECO CS-230 analyzer after acidification of the pulverized samples with HCl to remove inorganic carbon. Then, in order to remove residual HCl, the samples were washed using distilled water and further dried under vacuum (24 h at 60–80 °C). The carrying Standard was according to the Chinese Standard GB/T 19145-2022 "Determination of TOC in Sedimentary Rock".

Rock-Eval pyrolysis of pulverized samples was performed using an OGE-II instrument and following the Chinese Standard of GB/T18602-2017 "Rock Pyrolysis Analysis Method". The parameters including free HC content (S_1, mg HC/g rock) at 300 °C, remaining HC generative potential (S_2, mg HC/g rock) at between 300 and 600 °C, and T_{max} (temperature of maximum pyrolysis yield, ºC) were obtained during the process of heating.

2.4 Hydrocarbon Extraction, Fractionation, and Analysis

Before the test, the pulverized samples were used to obtain EOM by using a Soxhlet extractor system with a mixed solvent of methanol/dichloromethane. After 72 h, component separation was done using a silica gel-AlO chromatography, irrigating materials were normal hexane, benzene and hexanol. Gas chromatography-mass spectrometry (GC-MS) analysis was performed using an Agilent 6890GC/5975iMS, equipped with HP-5MS chromatographic column (60 m × 0.25 mm × 0.25 μm) according to the Chinese Standard of GB/T 18606-2012 "Determination of Sediments Biomarker by Gas Chromatography-Mass Spectrometry". During analysis, the initial temperature of the GC oven was 50 °C for 1 min, then programmed to raise to 120 °C at 20 °C/min, then to 310 °C for 25 min at 3 °C/min. Relative abundances of biomarkers were calculated from peak areas.

2.5 Measurement of Carbon Isotopes

$\delta^{13}C_{org}$ was performed using a Gas Isotope Ratio Mass Spectrometer (FLASH HT EA-MAT 253 IRMS instrument) system with analytical precision of ±0.5‰ and following the Chinese Standard of GB/T 18340.2-2010 "Organic Geochemical Analysis Method for Geological Samples-Part 2: Determination of Organic Carbon Stable Isotopic Component-Isotopic Mass Spectrometry". The $\delta^{13}C_{org}$ value was relative to the intentional PDB (Pee Dee Belemnite) standard, and the analytical error was ±0.1‰. The analysis conditions: gas chromatographic column was HP-PLOT Q column with 30 m; column ID was 0.53 mm; film thickness was 4 μm; heating temperature was from 40 to 160 ºC at a heating rate of 15 ºC/min, and then to 200 ºC at a heating rate of 5 ºC/min; 99.999% of carrier gas was He at a velocity of 1.3 mL/min.

2.6 Measurement of Maceral Composition and Vitrinite Reflectance

Firstly, the samples were cut along with the vertical direction of bedding; secondly, adding epoxy resin; finally, polishing the samples after laying for 24 h.

Identification and quantification of maceral composition were using microscopic properties (reflectance and structure) and surface area, respectively. Groups of sapropelinite and exinite were calculated using reflected fluorescent light and groups of inertinite and vitrinite were calculated using reflected white light fitted with an oil immersion objective. Measurement and classification of maceral composition were performed according to the Chinese Standard SY/T 6414-2014 "Maceral Analysis on Pol-

ished Surfaces of Whole Rocks" and SY/T 5125-2014 "Method of Determining Maceral Group Composition of Kerogen and Its Classification in Transmitted Light and Fluorescent Light Microscopy", respectively. The measurement of vitrinite reflectance (R_o) was calculated using a microscope photometer (MPV-SP).

3 RESULTS

3.1 Elemental and Carbon Isotopic Compositions

The TOC content, $\delta^{13}C_{org}$, EOM content, and elemental composition of kerogen for the source rocks are given in Table S1. The TOC content is 0.27 wt.%–9.64 wt.% (mean = 2.83 wt.%) and the $\delta^{13}C_{org}$ value ranges from -20.90‰ to -28.73‰ (-24.62‰ on average). The C, H, N, O and S elemental contents of kerogen are 59.27%–89.99% (81.95% on average), 2.88%–8.97% (5.94% on average), 1.24%–3.81% (2.51% on average), 2.00%–22.70% (8.46% on average) and 0.00%–15.58% (1.13% on average), respectively. Besides, the O/C and H/C atomic ratios as well as the C/N ratio of kerogen are 0.41–1.62 (mean = 0.88), 0.02–0.29 (mean = 0.08) and 22.09–65.25 (mean = 34.24), respectively.

The biogenic barium (Ba_{bio}) can be used to evaluate paleoproductivity, which is calculated as the following equation (Schoepfer et al., 2015; Ross and Bustin, 2009):

$$Ba_{bio} = Ba_{sample} - [Al_{sample} \times (Ba/Al)_{detrial}]$$

where Ba_{bio} and Ba_{sample} are the biogenic content and total concentration of Ba, and Al_{sample} is the total concentration of Al in the studied samples. In this study, $(Ba/Al)_{detrial}$ takes 0.006 8 based on the average related elements' concentration of the upper continental crust (McLennan, 2001). The concentrations and ratios of the major and trace elements discussed in this study are listed in Table S2.

3.2 Rock-Eval Pyrolysis

The S_1 and S_2 values are 0.07–10.62 mg HC/g rock and 0.08–46.68 mg HC/g rock, respectively. The hydrogen index (HI) value which is affected by the type and preservation of OM and, in turn, indicates the quality of source rocks, is 10–506 mg HC/g TOC. The T_{max} value ranges between 435 and 445 °C. The results of Rock-Eval pyrolysis are shown in Table S1.

3.3 Organic Petrology

The vitrinite group is dominant (> 50%) in some samples with the vitrinite reflectance being 0.59%R_o – 1.04%R_o (mean = 0.82%R_o) and the maceral composition in the rest samples is mainly composed of sapropelinite including sapropelic amorphogen, sapropelic alginate and sapropelic debris (66.97%–100%). The exinite and inertinite are 0%–26% and 0%–100%, respectively. The details of R_o value, maceral composition and the corresponding TI value are listed in Table S3.

3.4 Molecular Composition of Extractable Organic Matter

3.4.1 *n*-Alkanes and acyclic isoprenoids

The acyclic alkanes ranging between *n*-C_{12} and *n*-C_{35} are characterized by unimodal distribution in most samples (Figure 3a). The CPI (carbon preference index; Bray and Evans, 1961) and OEP (odd-to-even predominance; Peters and Moldowan, 1993) values vary from 1.02 to 1.99 and from 0.51 to 1.66, respectively (Table S4). Furthermore, the *n*-C_{17}/*n*-C_{23} and *n*-C_{17}/*n*-C_{27} ratios vary from 0.25 to 6.36 and from 0.57 to 10.58, respectively. Besides, the TAR (terrigenous/aquatic ratio; Bourbonniere and Meyers, 1996) value is 0.00–1.59 (Table S4) and Paq (submerged/floating macrophytes; Ficken et al., 2000) value is 0.53–1.00, respectively. The waxiness index (Σn-C_{21-31}/Σn-C_{15-20}; Peters et al., 2005) ranges between 0.20 and 2.70 (Table S4). The isoprenoid's abundances are smaller than its adjacent *n*-alkane's in most samples (i.e., the Pr/*n*-C_{17} and Ph/*n*-C_{18} ratios are 0.03–2.14 and 0.05–3.67 (Table S4), respectively) with the Pr/Ph ratio ranging between 0.71 and 4.02 (Table S4). In addition, the farnesane (*i*-C_{15}), *i*-C_{16} and nor-pristane (*i*-C_{18}) are also abundant in all samples (Figure 3a).

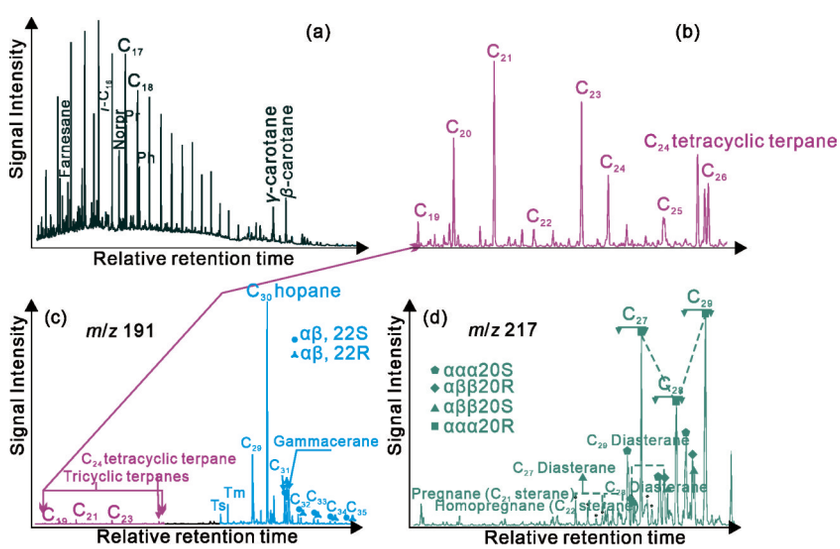

Figure 3. Biomarker characteristics for extracts of source rocks came from Well W9 in this study.

3.4.2 Terpanes

The terpane distribution is observed by the monitoring *m/z* 191 ion. The tricyclic terpanes (Tris), C_{24} tetracyclic terpane (Tet) and pentacyclic terpanes (hopanes) are widely distributed in all samples (Figure 3b).

The Tris ranging between C_{19} and C_{26} are observed in all samples, while extended Tris (C_{28} and C_{29}) can be detected in partial samples with the ETR ratio (extended Tris/Ts; Holba et al., 2001) ranging from 0.00 to 6.15 (Figure 3b). In the short Tris chains, the abundances of C_{22} and C_{24} Tris are smaller than the Tris before them with the C_{22}/C_{21} Tri of 0.07–0.21 and C_{24}/C_{23} Tri of 0.28–0.62, respectively. However, the abundance of C_{26} Tri is higher than that of C_{25} Tri in most samples with the C_{26}/C_{25} ratio of 0.96–16.61. The abundance of C_{24} Tet shows a large variation compared to C_{23} and C_{26} Tris with the C_{24} Tet/C_{23} Tri and C_{24} Tet/C_{26} Tri are 0.00–3.47 and 0.04–7.17, respectively (Table S5).

A series of hopanes, ranging from C_{27} to C_{35} except for C_{28}, including multiple stereoisomers are observed (Figure 3c). Except for the samples from Well W10, the hopane concentrations are greater than the Tris concentrations with the Tris/hopanes ratio being 0.06–0.76. The C_{30} hopane is greater than its adjacent C_{29} and C_{31} 22R hopanes with the C_{29}/C_{30} hopane ratio of 0.24–0.95 and C_{31} 22R/C_{30} hopane ratio of 0.09–0.47, respectively (Table S5). The low C_{35} hopane abundance is reflected by the HHI values of 0.00–0.06 (homohopane index, i.e., $C_{35}/\sum C_{31\text{-}35}$ 22S and 22R homohopanes; Peters and Moldowan, 1991) and C_{35}/C_{34} hopane ratio of 0–0.73, respectively (Table S5). Besides, gammacerane is detected with the gammacerane/C_{30} hopane ratio of 0.04–0.81 (Table S5). The 22S/(22S + 22R) ratios for C_{31} and C_{32} homohopane are 0.46–0.62 and 0.43–0.63, closing the equilibrium level, respectively (Table S5).

3.4.3 Steroids

The sterane distribution is observed by the monitoring *m/z* 217 ion (Figure 3d). The distribution characteristics of the steranes can be divided into two categories in the P_2p source rocks. The first category is characterized by the high abundances of C_{28} and C_{29} steranes, low abundances of C_{27} steranes (the C_{27}/C_{29} steranes ratio is 0.1–0.4 and C_{28}/C_{29} ratio is generally more than 0.6), and low or few abundances of diasteranes. The steranes distribution is "/" type (e.g., Well W6). The second category exhibits abundant C_{27} and C_{29} steranes with low C_{28} abundance, reflected in C_{27}/C_{29} ratios > 0.5 and exceptionally low C_{28}/C_{29} ratios (typically < 0.3). This category distribution forms an asymmetrical 'V' shape (Figure 3d), accompanied by significantly higher diasterane concentrations compared to the first category.

The C_{29} ααα 20S/(20S + 20R) and C_{29} ββ/(ββ + αα) ratios are 0.14–0.75 and 0.31–0.75 (Table S5), respectively. The C_{27} diasteranes/regular steranes ratio varies from 0.00 to 0.88 (Table S5). The pregnane is higher than homopregnane with the pregnane/homopregnane ratio of 1.15–3.20, and the $C_{21\text{-}22}/C_{27\text{-}29}$ steranes ratio is 0–0.70 (Table S5).

4 DISCUSSION

4.1 Source Rocks Characteristics

It is very important that HCs in samples were not contaminated by migrated HCs. S_1/TOC ratio can be used to determine whether indigenous HCs were contaminated by contaminants/migrated HCs (Hunt, 1996). Figure 4a clearly shows that the HCs are indigenous in all samples. However, four samples are anomalous (Figure 4b). This inconsistency might be a comprehensive result of the nature of kerogen type, variation in lithology, and state of OM preservation (Vaezian et al., 2014). For the two samples with relatively high PI values, it might be due to the migrated HCs. In poorly-drained systems, HCs discharged and then migrated and "contaminated" the same source rock unit by seeping from a thin layer of organic-rich rock into interbedded coarser-grained shales (Li et al., 2018; Chen and Jiang, 2016; Bernard and Horsfield, 2014; Reed et al., 2014; Bernard et al., 2012; Jarvie 2012). This is because the interbedded coarser-grained shales are organic-lean with less HC generation potential but contain more matrix pore space for migrated HCs and thereby show higher PI values (Cornford, 1998). Correspondingly, the two samples that have lower PI values may indicate the shale after HC expulsion.

4.1.1 Abundance and thermal maturity of organic matter

Both the $S_1 + S_2$ and EOM contents are positively related to TOC content (Figures 4c, 4d), indicating most of the samples are good-excellent source rocks (GP content > 6 mg/g; EOM content > 0.1%; and TOC content > 1.0%, respectively).

Both the T_{max} and R_o values illustrate the thermal maturity of OM in the source rocks are low mature and mature stages (Figure 5), which is consistent with the following molecular thermal maturity parameters. The parameters including the ratios of C_{31} and C_{32} hopane S/(S + R) (Figure 6a) align with the thermal maturity indicated by the C_{29} ααα 20S/(20S + 20R) and ββ/(ββ+αα) sterane ratios (Figure 6b), illustrating uniform low mature and mature stages.

4.1.2 Origin of organic matter

Firstly, a bacterial contribution to the OM is evidenced by the occurrence of branched alkanes (Shiea et al., 1990) and farnesane which is an indicator of green sulfur bacteria (Summons and Powell, 1987). Besides, short-chain Tris (C_{19} and C_{20}) are believed to be related to bacteria (Marynowski et al., 2000). Hopanes mainly derive from hopane polyols found in bacterial membranes (Ourisson and Albrecht, 1992; Ourisson and Rohmer, 1992) and are generally used as a biomarker for aerobic bacteria (Peters et al., 2005). The high concentration of hopanes is evidence of bacteria as well (Figure 3c).

Secondly, aquatic plants including saltwater algae, fresh algae, Sphagnum moss species, submerged macrophytes, phytoplankton (e.g., Nymphaea), and aquatic pollen taxa are important OM sources. *n*-Alkanes with

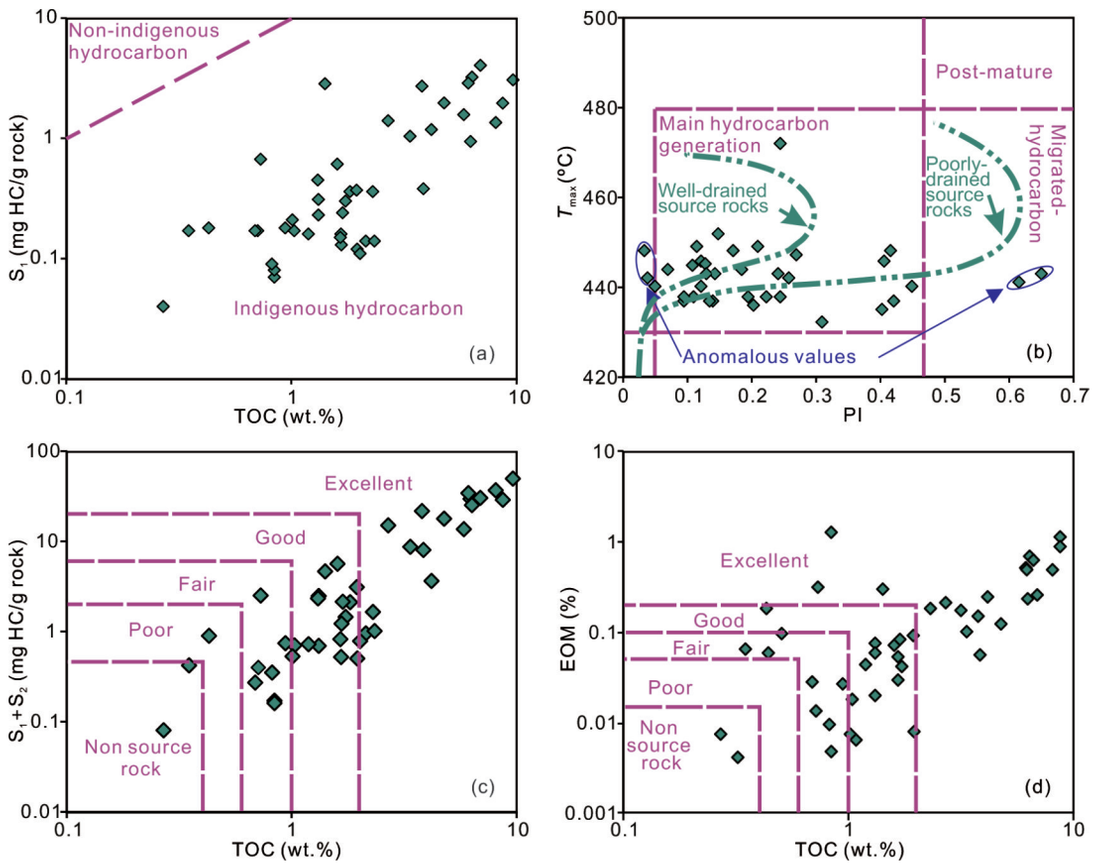

Figure 4. Plots of (a) S_1 *versus* TOC and of (b) T_{max} *versus* PI (modified after Abdullah et al., 2017) for identifying the migration index as well as of TOC *versus* each of (c) $S_1 + S_2$ and (d) EOM for showing hydrocarbon generation potential of the P_2p source rocks in the Wucaiwan sag, Junggar Basin. Note: TOC = total organic carbon, wt.%; S_1 = volatile hydrocarbon (HC) content, mg HC/g rock; S_2 = remaining HC generative potential, mg HC/g rock; GP = genetic potential ($S_1 + S_2$), mg HC/g rock; PI = production index (S_1/GP), dimensionless; T_{max} = temperature of maximum pyrolysis yield, ºC; EOM = extractable organic matter, %.

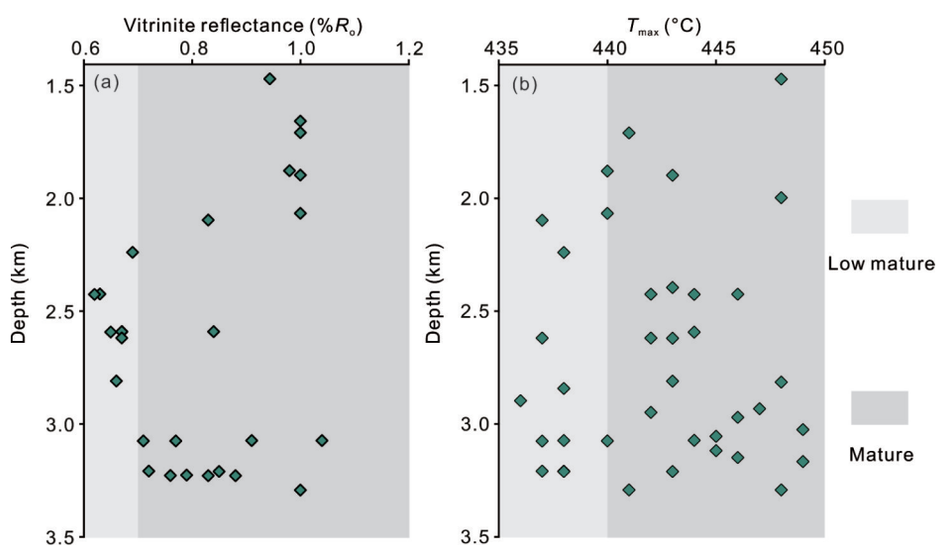

Figure 5. Plots of (a) R_o and (b) T_{max} *versus* buried depth showing organic matter thermal maturity stages for the samples from the P_2p source rocks in the Wucaiwan sag, Junggar Basin. Note: R_o = vitrinite reflectance, %R_o.

low carbon numbers (e. g., *n*-$C_{12} - C_{18}$) represent typical OM input from algae and phytoplankton (Luo et al., 2016; Meyers, 1997; Table S4). *n*-Alkanes with peak carbon of C_{17} or C_{18} (Table S4) typically originate from cyanobacteria and algae (Riboulleau et al., 2007; Hunt, 1996). Middle-chain *n*-alkanes (*n*-C_{21-25}) originate from aquatic plants (Ficken et al., 2000), especially with relatively high concentrations of *n*-C_{23} and *n*-C_{25} alkanes (Huang et al.,

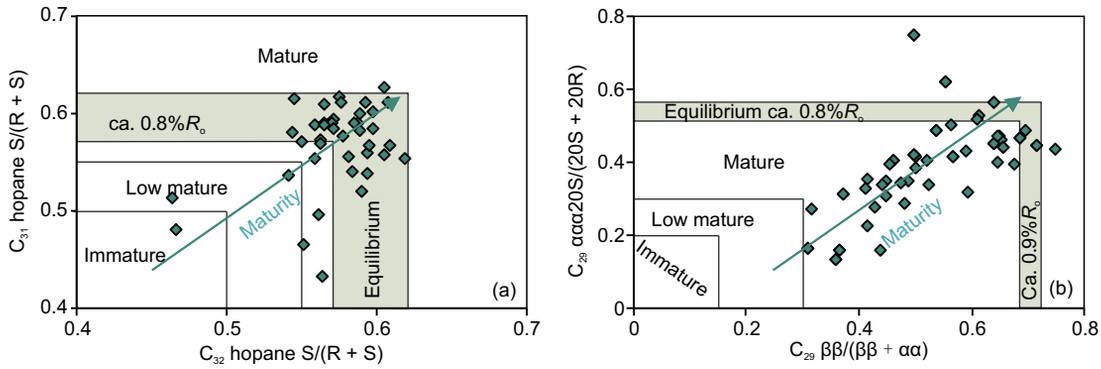

Figure 6. Molecular indicators of thermal maturity of OM by (a) 22S/(22S + 22R) C_{31} homohopane *versus* 22S/(22S + 22R) C_{32} homohopane and (b) C_{29} ααα 20S/(20S + 20R) *versus* C_{29} ββ/(ββ + αα) sterane isomerization for the P_2p source rocks in the Wucaiwan sag, Junggar Basin. Equilibrium = equilibration levels equivalent to vitrinite reflectance values (data from Qiao et al., 2021a; Peters et al., 2005).

1999) corresponding to high concentrations of aquatic pollen taxa, Nymphaea (Coetzee, 1967), Sphagnum moss species (Bingham et al., 2010; Nichols et al., 2006), fresh-water algae (Riboulleau et al., 2007). Moreover, Paq > 0.4 indicates submerged/floating fresh-water macrophytes input (Ficken et al., 2000) and moderate ETR values may be related to an algal contribution from primary producers (Volk et al., 2005). The high C_{27} sterane abundance further suggests an attribution of microalgae OM in the samples (Volkman, 2003; Huang and Meinschein, 1979). The Lucaogou Formation which mainly developed in the southern Junggar Basin deposited with the P_2p Formation at the same time (Luo et al., 2018). Microbial fossils that might from methanotrophic archaea and sulfate-reducing bacteria have been observed by Xie et al. (2015) in the Lucaogou Formation.

Thirdly, long-chain *n*-alkanes with obvious odd carbon predominance in *n*-C_{23}–C_{27} in most samples are generally attributed to higher plants (Eglinton and Calvin, 1967) and presences of C_{27}, C_{29}, and C_{31} *n*-alkanes indicate that land plant epicuticular waxes are an important source of geolipids to the source rocks (Meyers, 1997). Besides, the OM sourced from land plants is further supported by the higher abundances of C_{24}Tet and C_{29} steranes. The OM derived from higher plants can also be supported by the Permian palynofloras dominated by gymnospermous pollen, such as conifers and ferns, in the Junggar Basin (Zhu et al., 2005).

In summary, based on the above evidence, the OM origin is a mixture of algal-bacterial-land plants, which is further supported by the combination of low to middle C_{24}/C_{23} Tri and low C_{22}/C_{21} Tri ratios (Adegoke et al., 2014). Moreover, a series of indicators reflecting the relative contribution of each component, such as the *n*-C_{17}/*n*-C_{23} ratio indicating the relative contribution of marine/saltwater and fresh-water algae (Riboulleau et al., 2007), *n*-C_{17}/*n*-C_{27} ratio, TAR and waxiness values suggesting the relative contribution of bacterial-aquatic and terrigenous inputs (Bourbonniere and Meyers, 1996; Connan and Cassou, 1980), steranes/hopanes ratio suggesting the relative contribution of plant and microorganism (Peters et al., 2005), and distribution of *n*-alkanes, show great variations, indicating the OM composition is complicated**.** A ternary diagram showing the distribution of the C_{27}, C_{28} and C_{29} steranes and paleodepositional environments of the P_2p source rocks is shown in Figure 7, indicating the OM sources were mixed by phytoplankton, land plants and bacteria under terrestrial, bay and estuary environments. Additionally, the first category samples are mainly concentrated on the margin of the sag, such as Well W6, indicating the proportion of aquatic organisms was relatively small and that of terrestrial plants was relatively large, while the second category which suggestive of an increase in aquatic organisms and a decrease in terrestrial land plants compared with the first category mainly distributed in the center of the sag, such as Well W9 (Figure 3d).

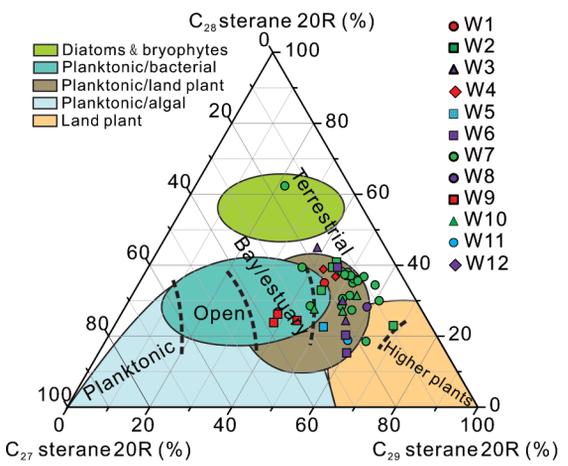

Figure 7. Ternary diagram showing the distribution of C_{27}, C_{28} and C_{29} steranes and depositional environment of the P_2p source rocks in the Wucaiwan sag, Junggar Basin (modified after Moldowan et al., 1985; Huang and Meinschein, 1979).

The kerogen type in the source rocks can be interpreted as types II and III kerogens with a small number of Type I kerogen based on the results from Rock-Eval pyrolysis (Figures 8a and 8b) and atomic ratios (Figure 8c), which indicates a mixture of minor planktonic-bacterial inputs and major terrestrial higher plants. The maceral composition shows a similar result (Table S3). It should

be noted that Figures 8a and 8b show smaller contributions of Type I kerogen in the studied samples in comparison to Figure 8c. This might be due to two reasons. On the one hand, the thermal maturity of OM effect on S_2 values is not considered in Figure 8b. On the other hand, hydrogen in H/C atomic ratio means the total hydrogen (including both S_1 and S_2) present in samples (including hydroxyl), while HI measures only detectable material released by pyrolysis of OM and does not account for the hydrogen content in the thermal extract (S_1). The high S_1 value corresponding to about 3.20%–65.03% of the total HCs released during pyrolysis might add to the elevated H/C atomic ratio at a moderate HI value. Furthermore, the $\delta^{13}C_{org}$ value is usually consistent with an ecosystem dominated by terrestrial C_3 plants (Figure 9a; Robinson and Hesselbo, 2004; Freeman and Colarusso, 2001). In addition, although C/N ratio of kerogen is easily affected by other factors, the high C/N ratio ranging from 21.65 to 76.13 (mean = 39.35) indicates that the OM of the source rocks was dominated by terrestrial C_3 plants with little freshwater dissolved organic carbon (DOC) which is a mixture of higher plants and phytoplankton in lacustrine environments (Figure 9a; Lamb et al., 2006; Hedges et al., 1997; Meyers, 1994).

4.2 Paleodepositional Environment

In lake systems, salinity is very important for the composition of aquatic organism community (Qiao et al., 2021b; Romero-Viana et al., 2012). Generally, C_{31} 22R/C_{30} hopane ratio of > 0.25 indicates marine situations, while of < 0.25 refers to lacustrine environments (Peters et al., 2005). The C_{31} 22R/C_{30} hopane ratio indicates the P_2p source rocks were deposited in a lacustrine environment, which is consistent with the C_{26}/C_{25} Tri and C_{34}/C_{35} hopane ratios of > 1, low C_{22}/C_{21} and C_{24}/C_{23} Tri ratios, and low HHI values (Peters et al., 2005; Sinninghe Damsté et al., 1995; Peters and Moldowan, 1991). Besides, the regular decreasing distribution from C_{31} to C_{35} hopanes in the samples illustrates clastic facies (Figure 3c; Waseda and Nishita, 1998). In addition, the C_{29}/C_{30} hopane ratio of < 1 indicates that the source rocks are clay-rich source rocks (Gürgey, 1999). The clay-rich envi-

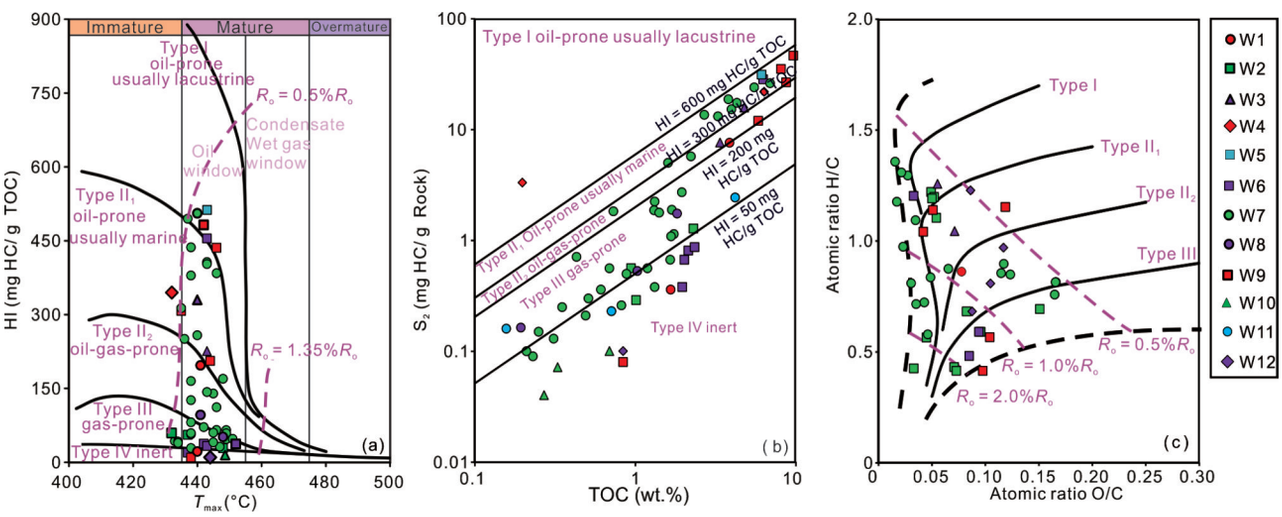

Figure 8. Plots of (a) HI *versus* T_{max} values (modified after Cornford et al., 1998), of (b) S_2 value *versus* TOC content (modified after Langford and Blanc-Valleron, 1990) and of (c) O/C *versus* H/C atomic ratios (modified after Peters, 1986), showing kerogen types for the samples from the P_2p source rocks in the Wucaiwan sag, Junggar Basin. Note: HI = hydrogen index (S_2 × 100/TOC), mg HC/g TOC.

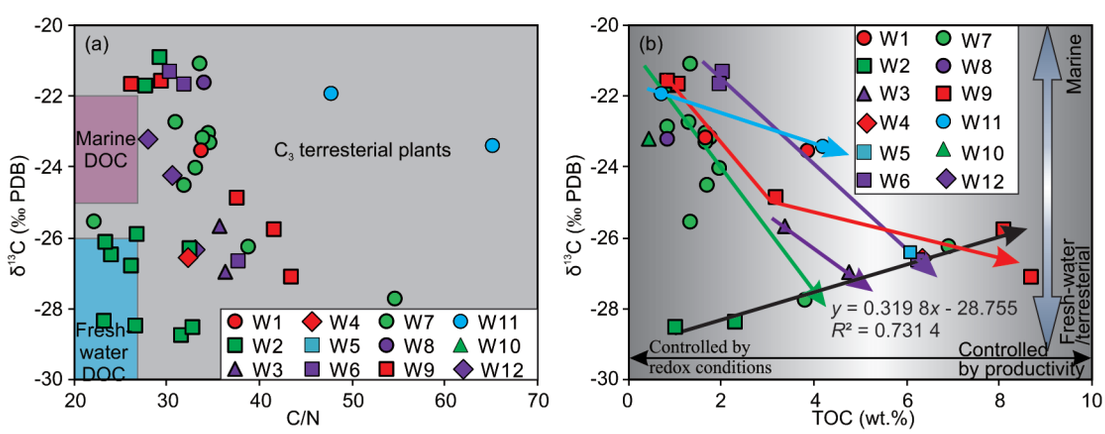

Figure 9. Kerogen carbon isotope *versus* (a) C/N ratio and *versus* (b) TOC content (after Lamb et al., 2006) for the P_2p source rocks in the Wucaiwan sag, Junggar Basin.

ronment can be further supported by the high C_{27} diasteranes/regular steranes ratio compared to the C_{21-22}/C_{27-29} steranes ratio (Figure 10; Zheng et al., 2022; Qiao et al., 2021a). The non-marine depositional environment is further indicated by the high Pr/*n*-C_{17} ratio of > 0.6, appearance of *β*-Carotane (Figure 3b), low steranes/hopanes ratio of < 1, and low abundance of C_{28} sterane (Peters et al., 2005). Based on the biomarker parameters, the study area was a typical clay-rich lacustrine environment without seawater intrusion. The lacustrine environment with large variation in salinity is further supported by the low Tris/C_{30} αβ hopane ratios as well as low pregnane and homopregnane compared to steranes (< 0.1) in most samples (Qiao et al., 2021b; Peters et al., 2005; Requejo et al., 1997; Kruge et al., 1990; ten Haven et al., 1985) (Figure 11a). The lacustrine environment was also interpreted in the Shazhang fault-fold zone (Zhang et al., 2021) and in the Shishugou sag based on lithological analyses and data of source rocks from Well Shishu 1 (Kuang et al., 2012).

The same result can be deduced from the existence of gammacerane which is inductive in the stratification of water columns (Peters et al., 2005; Sinninghe Damsté et al., 1995). Gammacerane originates from tetrahymanol (ten Haven et al., 1989), synthesized by bacterivorous ciliates that feed at the interface between anoxic and oxic zones in stratified water columns (Sinninghe Damsté et al., 1995). The concentrations of gammacerane indicate the stratification of water columns in a lacustrine environment. Stratification of water columns includes thermal stratification and saline stratification (Peters et al., 2005). Gammacerane may occur in a longitudinal direction of the high saline water with the above inferences on the reasons for the change of salinity. The wide range of gammacerane/C_{30} hopane ratio indicates the variation in salinity.

In addition to paleosalinity, the paleoredox condition is another important factor affecting OM preservation (Qiao et al., 2021a, b). Pr/Ph ratio is widely used as a good proxy for paleoredox situations (Zhang et al., 2020; ten Haven et al., 1987; Didyk et al., 1978). Pr/Ph < 1 (related to increasing algae input) indicates anoxic environments, and Pr/Ph > 3 indicates oxic situations with a significant contribution of terrigenous plants and aquatic organisms (Didyk et al., 1978). The higher Pr/Ph ratio, the more oxidation degree, and the shallower water columns in paleoenvironments (marshes, wetlands, paralic etc.). Only one of the studied sample showing Pr/Ph of > 3 indicates reducing situations with few oxic environments (Table S4; Peters et al., 2005; Didyk et al., 1978), which are further demonstrated by the plot of Pr/*n*-C_{17} *vs*. Ph/*n*-C_{18} (Figure 11b).

4.3 Factors Controlling Organic Matter Accumulation

Paleoredox conditions and paleoproductivity are the most important controlling factors on OM accumulation in OM-rich sediments even though distribution, enrichment and development of OM-rich sediments are the results of a series of complex physical and chemical processes (Liu et al., 2021). Although the regional/periodic oxic condition was not in favor of OM preservation, the moderate biological productivity in the sag was the material basis for developing OM-rich deposits (Wu et al., 2022a; Demaison and Moor, 1980; Hunt, 1979). Nutrient elements, such as Cu and Ni, combine with OM or form organic complex compounds to deposit, and redox conditions have little effect on them (Nameroff et al., 2004; Piper and Perkins, 2004), so they can be used to evaluate paleoproductivity. In order to eliminate the input effect of terrigenous clastic materials, Ni and Cu concentrations compared to Al concentration are used to evaluate paleo-

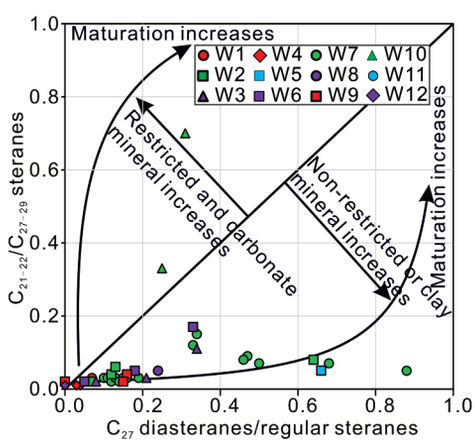

Figure 10. Plot of C_{21-22}/C_{27-29} steranes *versus* C_{27} diasteranes/regular steranes of the P_2p source rocks in the Wucaiwan sag, Junggar Basin (modified after Qiao et al., 2021a; Wang et al., 2015).

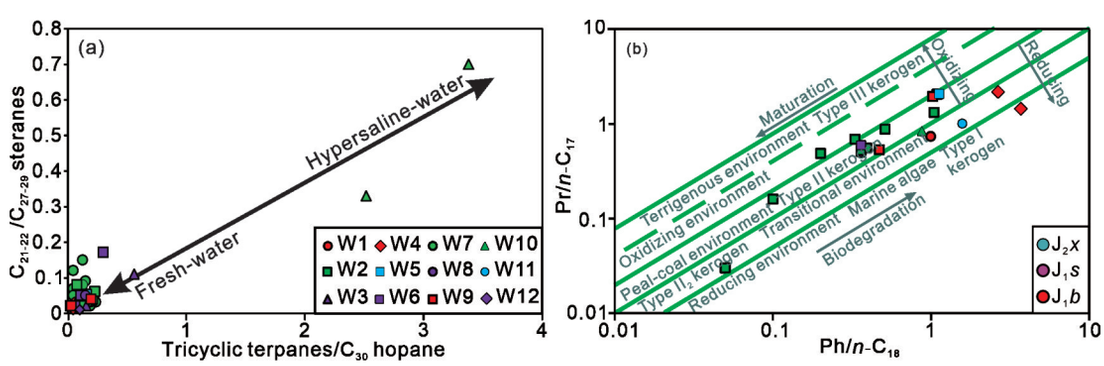

Figure 11. Plots of (a) tricyclic terpanes/C_{30} hopane *versus* C_{21-22} steranes/C_{27-29} steranes and (b) Ph/*n*-C_{18} *versus* Pr/*n*-C_{17} (modified after Peters et al., 2005 and Shanmugam, 1985), showing depositional conditions of the P_2p source rocks in the Wucaiwan sag, Junggar Basin.

productivity in this study. The Ni/Al and Cu/Al ratios are 2.21 × 10^{-4}–9.16 × 10^{-4} (avg. 5.62 × 10^{-4}) and 2.47 × 10^{-4}–26.01 × 10^{-4} (avg. 10.35 × 10^{-4}), respectively, which is similar to the ratios of the Wufeng and Longmaxi shales (i.e., Ni/Al ratios are 4.04 × 10^{-4}–54.63 × 10^{-4} with an average value of 11.96 × 10^{-4} and Cu/Al ratios are 3.35 × 10^{-4}–34.33 × 10^{-4} with an average value of 8.60 × 10^{-4}) (Zhao et al., 2016), indicating an overall moderate paleoproductivity level which exactly covers from low to high levels in comparison to the high upwelling productivity offshore Peruvian (Ni/Al ratios are 1.91 × 10^{-4}–55.35 × 10^{-4} with an average value of 23.38 × 10^{-4} and Cu/Al ratios are 8.7 × 10^{-4}–24.5 × 10^{-4} with an average value of 15.2 × 10^{-4} on average) (Böning et al., 2004), in comparison to the high productivity in the Lower Cambrian Niutitang shale (Ni/Al ratios are 2.58 × 10^{-4}–161.44 × 10^{-4} with an average value of 41.15 × 10^{-4} and Cu/Al ratios are 3.54 × 10^{-4}–137.33 × 10^{-4} with an average value of 41.01 × 10^{-4}) (Tan et al., 2021), and in comparison to the low paleoproductivity in the Longtan Formation where Ni/Al ratio is 1.80 × 10^{-4}–5.11 × 10^{-4} (avg. 3.17 × 10^{-4}) and Cu/Al ratio is 1.23 × 10^{-4}–3.66 × 10^{-4} (avg. 2.84 × 10^{-4}) (Wu et al., 2022b). Compared to Cu and Ni, Ba escapes easily in reducing environments (Schoepfer et al., 2015). So, the reducing condition (Figure 11b) might result in the underestimation of the paleoproductivity based on Ba. However, the Ba_{bio} of 0 ppm–724.80 ppm (372.68 ppm on average) also indicates an overall moderate paleoproductivity in comparison to that of 38 ppm–8 264 ppm (avg. 1 521 ppm) in the Lower Cambrian Niutitang shale (Tan et al., 2021). Such large heterogeneities in paleoproductivity proxies are relatively common in terrestrial lake sediments. This is because scales of lacustrine basins with weak fragile ecosystems are much smaller than those of marine settings, and terrestrial lakes are easily affected by external factors (e.g., freshwater and terrestrial OM inputs), leading to the variations of issues including OM types, salinities of water columns and redox conditions of benthic water, etc. In this study, all related parameters mentioned above, e.g., TOC contents, show great variations. As a result, the paleoproductivity and controlling factors for OM in lacustrine settings are more complex and variable.

The relative importance of paleoredox condition and paleoproductivity as controlling factors on OM preservation can be evaluated via the relationship between TOC content and $\delta^{13}C_{org}$ value. Where paleoproductivity is the controlling factor, $\delta^{13}C_{org}$ value is positively correlated to TOC content; where OM preservation is controlled by paleoredox conditions, the relationship generally shows a negative correlation (Qiao et al., 2022, 2020; Huang et al., 2017; Curiale and Gibling, 1994; Freeman et al., 1994, 1990; Hollander and McKenzie, 1991).

The Wucaiwan sag exhibited a weak weathering intensity due to the aridity/cold paleoclimate condition during the Permian glacial stage (Zhu et al., 2005; González, 1990) and resulting in a weak dilution of terrestrial inputs. The relatively cold and arid paleoclimate conditions were beneficial to brackish-water conditions (high gammacerane abundances for most samples in Figure 12). Similar paleodepositional conditions can be observed in the Qaidam Basin (Qiao et al., 2021b). The water stratification was brackish-water condition superposed by periodic/occasional fresh-water influx (e.g., rainfall and river drain,

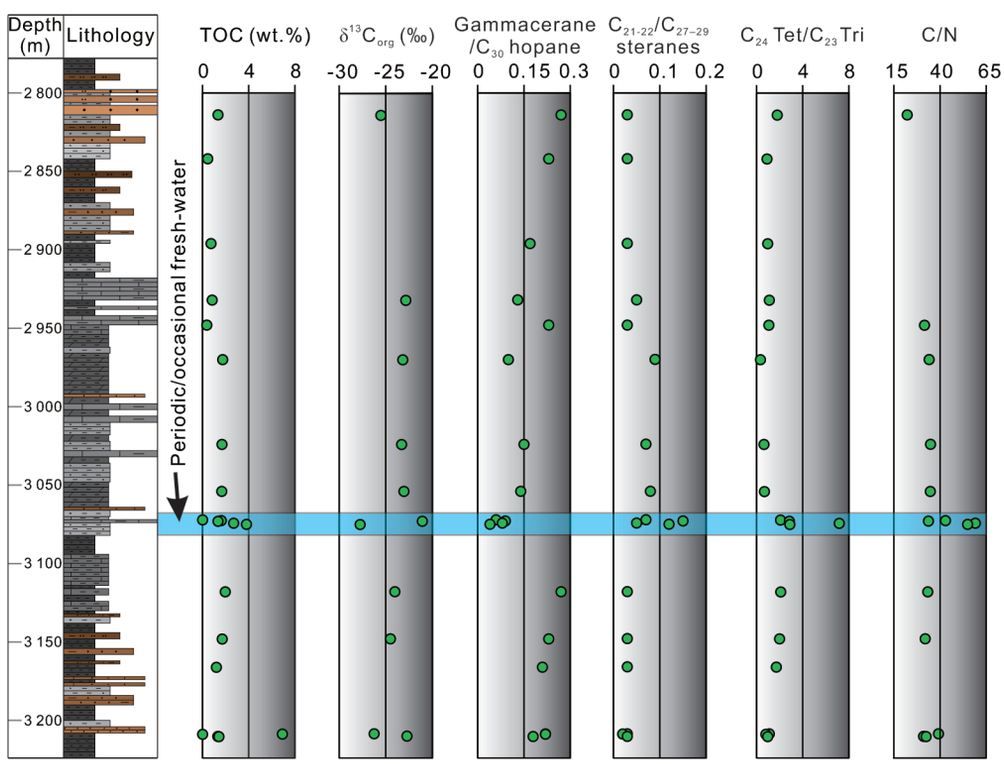

Figure 12. Stratigraphic distributions of lithology, TOC content, and geochemical data of the P_2p Formation from Well W7.

which can be supported by the higher C_{21-22}/C_{27-29} steranes and lower $\delta^{13}C_{org}$ value at around 3 070 m; Figure 12), which resulted in fresh-water condition and well oxygenating in the water column during overturn processes (the unusually lower gammacerane and $\delta^{13}C_{org}$ values at around 3 070 m; Figure 12). Along with fresh-water influx, plenty of terrestrial plants were transported in the sag which resulted in a relatively large proportion of terrestrial higher plants in the source rocks (the unusually high 24 Tet/C_{23} Tri and C/N ratios at around 3 070 m; Figure 12). During periodic/occasional fresh-water influx periods with plenty of terrestrial plants inputs, the paleoredox conditions of the sag were relatively oxic in the shallow fresh-water which experienced strong oxidation and decomposition of OM, therefore were not conducive for the OM preservation. However, the primary productivity made up for this deficiency, and was the main controlling factor in the samples with high TOC content. A suitable supply from terrestrial inputs can promote the biotic paleoproductivity during periodic/occasional fresh-water influx periods (relatively high TOC contents at around 3 070 m; Figure 12), and a relatively high sedimentation rate can reduce the oxidation and decomposition times of OM. The excess terrestrial OM input compensated for the preservation of OM under adverse oxidation conditions, which can be supported by the positive relationship between TOC and $\delta^{13}C_{org}$ value for the samples with $\delta^{13}C_{org}$ value < -26‰ which indicates fresh-water conditions and terrestrial environments (Mackie et al., 2005; Andrews et al., 2000; Figure 9b). The periodic/occasional fresh-water influx not only led to the variation of paleoredox conditions and paleosalinity but also resulted in the variation in the OM composition (Figure 12 at a depth around 3 070 m and Figure 13a). By contrast, the terrestrial higher plants proportion decreased, and the aquatic organisms proportion increased in the sag during the periods without fresh-water inputs (Figure 13b). This setting was characterized by the lower TOC content, reducing and high salinity conditions. This case corresponds to the $\delta^{13}C_{org}$ value being greater than the -26‰ area in Figure 9b where a negative relationship between the TOC content and $\delta^{13}C_{org}$ value occurred, indicating the redox condition was more important for the preservation of OM accumulation due to the decrease of the biotic source and reducing conditions. It should be noted that the whole study area developed lacustrine source rocks without seawater intrusion.

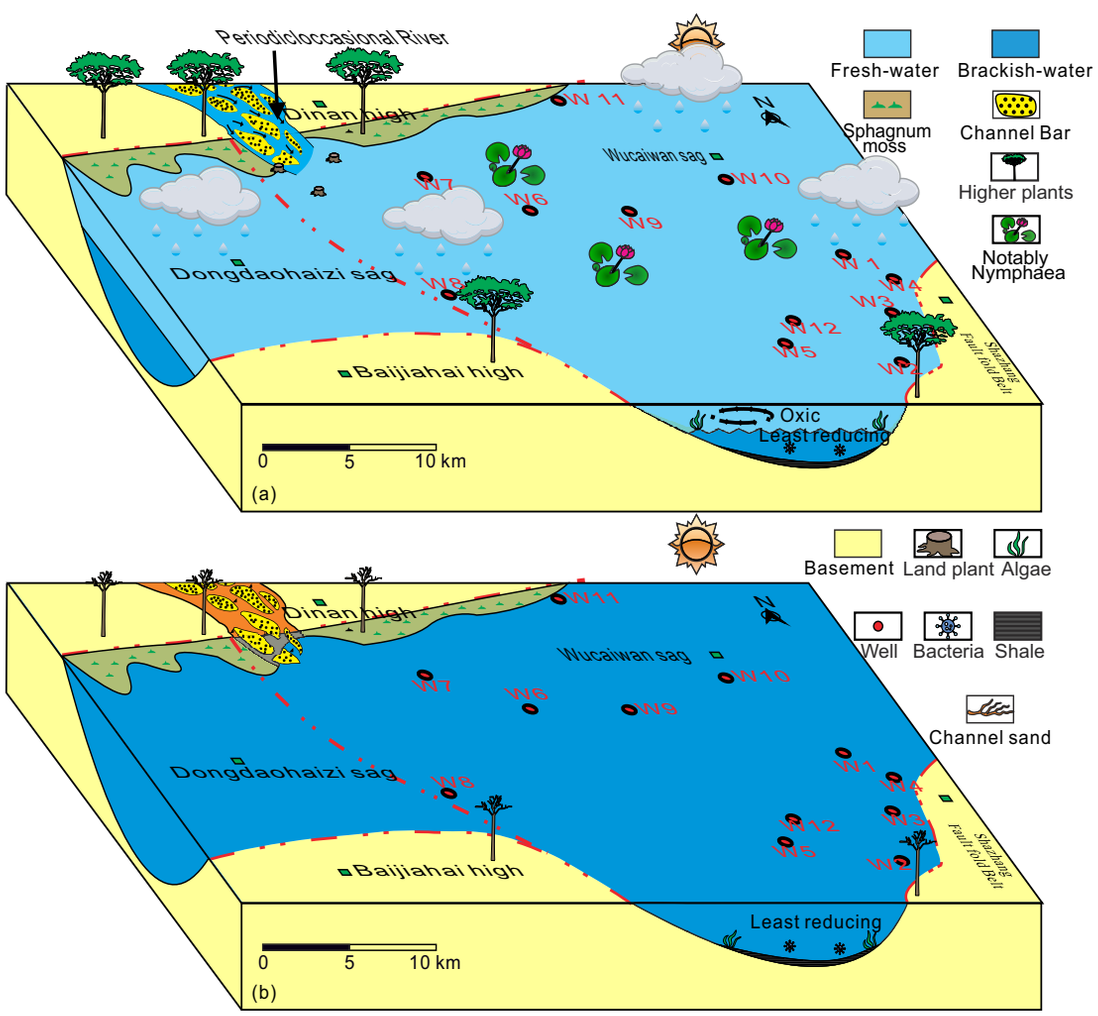

Figure 13. Paleodepositional mode patterns of the P_2p Formation (a) with the periodic/occasional fresh-water influx and (b) without fresh-water inputs in the Wucaiwan sag, Junggar Basin.

Briefly, the Wucaiwan sag developed reducing environment in benthic water and brackish-water column, which were in favor of OM accumulation. However, this situation can be superposed by periodic/occasional fresh-water influx resulting in fresh-water condition and well oxygenating in the water column during overturn processes, which was not in favor of OM preservation. Nevertheless, the input of fresh-water with more terrestrial high plants made up for this deficiency and lead to the high OM contents in the studied area of OM.

5 CONCLUSIONS

Based on the comprehensive study of carbon isotopic composition, biomarker characteristics, element compositions of kerogen and whole rock, organic petrology, and Rock-Eval data, the hydrocarbon potential, development conditions and factors controlling the formation of the Permian Pingdiquan (P_2p) source rocks in the Wucaiwan sag are interpreted.

(1) The P_2p Formation developed both well-drained and poorly-drained lacustrine source rocks. The hydrocarbon potential is good-excellent with low to middle thermal mature stages of organic matter.

(2) The organic matter sources were mixed, including plenty of terrestrial C_3 higher plants and some aquatic organisms including aerobic bacteria, green sulfur bacteria, saltwater and fresh algae, Sphagnum moss species, submerged macrophytes, Nymphaea, and aquatic pollen taxa. The proportion of terrestrial higher plants decreased and that of aquatic organisms increased from margin to center of the sag.

(3) The source rocks were deposited under brackish-water and reducing conditions with the periodic/occasional fresh-water influx (e.g., rainfall and river drain) resulting in fresh-water conditions and well oxygenating in the water column during overturn processes.

(4) The paleoproductivity was the main controlling factor for the accumulation of organic carbon in the samples that occurred fresh-water influx. However, during the intervals of the fresh-water influx, the redox conditions showed a more important controlling factor in the organic matter accumulation due to the decrease of the biotic source.

ACKNOWLEDGMENTS

I would like to express my gratitude to all those who have helped me during the writing of this publication. Special thanks will be extended to the strong support (samples and data) from Cainan Oilfield. This study was financially supported by the National Natural Science Foundation of China (NSFC) (No. 42202154), and the Science Foundation of China University of Petroleum, Beijing (No. ZX20220074). The final publication is available at Springer via https://doi.org/10.1007/s12583-022-1804-0.

Electronic Supplementary Materials: Supplementary materials (Tables S1–S5) are available in the online version of this article at https://doi.org/10.1007/s12583-022-1804-0.

Conflict of Interest

The authors declare that they have no conflict of interest.

REFERENCES CITED

Abdullah, W. H., Togunwa, O. S., Makeen, Y. M., et al., 2017. Hydrocarbon Source Potential of Eocene–Miocene Sequence of Western Sabah, Malaysia. *Marine and Petroleum Geology*, 83: 345–361. https://doi.org/10.1016/j.marpetgeo.2017.02.031

Adegoke, A. K., Abdullah, W. H., Hakimi, M. H., et al., 2014. Geochemical Characterisation of Fika Formation in the Chad (bornu) Basin, Northeastern Nigeria: Implications for Depositional Environment and Tectonic Setting. *Applied Geochemistry*, 43(4): 1–12. https://doi.org/10.1016/j.apgeochem.2014.01.008

Andrews, J. E., Samways, G., Dennis, P. F., et al., 2000. Origin, Abundance and Storage of Organic Carbon and Sulphur in the Holocene Humber Estuary: Emphasizing Human Impact on Storage Changes. *Geological Society, London, Special Publications*, 166(1): 145–170. https://doi.org/10.1144/gsl.sp.2000.166.01.09

Bai, H., Pang, X. Y., Kuang, L., et al., 2017. Depositional Environment, Hydrocarbon Generation and Expulsion Potential of the Middle Permian Pingdiquan Source Rocks Based on Geochemical Analyses in the Eastern Junggar Basin, NW China. *Australian Journal of Earth Sciences*, 64(4): 497–518. https://doi.org/10.1080/08120099.2017.1310139

Bernard, S., Horsfield, B., 2014. Reply to Comment on "Formation of Nanoporous Pyrobitumen Residues during Maturation of the Barnett Shale (Fort Worth Basin)". *International Journal of Coal Geology*, 127: 114–115. https://doi.org/10.1016/j.coal.2014.01.005

Bernard, S., Wirth, R., Schreiber, A., et al., 2012. Formation of Nanoporous Pyrobitumen Residues during Maturation of the Barnett Shale (Fort Worth Basin). *International Journal of Coal Geology*, 103: 3–11. https://doi.org/10.1016/j.coal.2012.04.010

Bian, W. H., Hornung, J., Liu, Z. H., et al., 2010. Sedimentary and Palaeoenvironmental Evolution of the Junggar Basin, Xinjiang, Northwest China. *Palaeobiodiversity and Palaeoenvironments*, 90(3): 175–186. https://doi.org/10.1007/s12549-010-0038-9

Bingham, E. M., McClymont, E. L., Valiranta, M., et al., 2010. Conservative Composition of *n*-Alkane Biomarkers in Sphagnum Species: Implications for Palaeoclimate Reconstruction in Ombrotrohic Peat Bogs. *Organic Geochemistry*, 41(2): 214–220. https://doi.org/10.1016/j.orggeochem.2009.06.010

Böning, P., Brumsack, H. J., Bottcher, M. E., et al., 2004. Geochemistry of Peruvian Near-Surface Sediments. *Geochimica et Cosmochimica Acta*, 68(21): 4429–4451. https://doi.org/10.1016/j.gca.2004.04.027

Bourbonniere, R. A., Meyers, P. A., 1996. Anthropogenic Influences on Hydrocarbon Contents of Sediments Deposited in Eastern Lake Ontario since 1800. *Environmental Geology*, 28 (1): 22–28. https://doi.org/10.1007/s002540050074

Bray, E. E., Evans, E. D., 1961. Distribution of n-Paraffins as a Clue to Recognition of Source Beds. *Geochimica et Cosmochimica*

Acta, 22(1): 2–15. https://doi.org/10.1016/0016-7037(61)90069-2

Cao, Z., Gao, J., Liu, G. D., et al., 2017. Investigation of oil Potential in Saline Lacustrine Shale: A Case Study of the Middle Permian Pingdiquan Shale (Lucaogou Equivalent) in the Junggar Basin, Northwest China. *Energy Fuels*, 31(7): 6670–6688. https://doi.org/10.1021/acs.energyfuels.7b00294

Caplan, M. L., Bustin, R. M., 1999. Palaeoceanographic Controls on Geochemical Characteristics of Organic-Rich Exshaw mudrocks: Role of Enhanced Primary Production. *Organic Geochemistry*, 30(2–3): 161–188. https://doi.org/10.1016/S0146-6380(98)00202-2

Carroll, A. R., Brassell, S. C., Graham, S. A., 1992. Upper Permian Lacustrine Oil Shales, Southern Junggar Basin, Northwest China. *American Association of Petroleum Geologists Bulletin*, 76: 1874–1902. https://doi.org/10.1306/bdff8b0a-1718-11d7-8645000102c1865d

Chen, Z. H., Jiang, C. Q., 2016. A Revised Method for Organic Porosity Estimation in Shale Reservoirs Using Rock-Eval Data: Example from Duvernay Formation in the Western Canada Sedimentary Basin. *American Association of Petroleum Geologists Bulletin*, 100(3): 405–422. https://doi. org/10.1306/08261514173

Chen, Z. Q., Liao, Z. T., Liu, L. J., 2015. Correction of Two Upper Paleozoic Stratigraphic Units in the Tianshan Mountains Region, Xinjiang Uygur Autonomous Region and Implications on the Late Paleozoic Evolution of Tianshan Tectonic Complex, Northwest China. *Journal of Paleogeography*, 4(4): 359–372. https://doi.org/2095-3836(2015)4:42.0.tx;2-5

Coetzee, J. A., 1967. Pollen Analytical Studies in East and Southern Africa. *Palaeoecology of Africa*, 3: 1–146

Connan, J., Cassou, A. M., 1980. Properties of Gases and Petroleum Liquids Derived from Terrestrial Kerogen at Various Maturation Levels. *Geochimica et Cosmochimica Acta*, 44(1): 1–23. https://doi.org/10.1016/0016-7037(80)90173-8

Cornford, C., Gardner, P., Burgess, C., 1998. Geochemical Truths in Large Data Sets. I: Geochemical Screening Data. *Organic Geochemistry*, 29 (1–3): 519–530. https://doi.org/10.1016/s0146-6380(98)00189-2

Curiale, J. A., Gibling, M. R., 1994. Productivity Control on Oil Shale Formation—Mae Sot Basin, Thailand. *Organic Geochemistry*, 21: 67–89. https://doi:10.1016/0146-6380(94)90088-4

Demaison, G. J., Moore, G. T., 1980. Anoxic Environments and Oil Source Bed Genesis. *American Association of Petroleum Geologists Bulletin*, 64(8): 1179–1209. https://doi. org/10.1306/2f91945e-16ce-11d7-8645000102c1865d

Didyk, B. M., Simoneit, B. R. T., Brassell, S. C., et al., 1978. Organic Geochemical Indicators of Paleoenvironmental Conditions of Sedimentation. *Nature*, 272: 216–222. https://doi. org/10.1038/272216a0

Eglinton, G., Calvin, M., 1967. Chemical Fossils. *Scientific American*, 216(1): 32–43. https://doi.org/10.1038/scientificamerican0167-32

Ficken, K. J., Li, B., Swain, D. L., et al., 2000. An *n*-Alkane Proxy for the Sedimentary Input of Submerged/Floating Freshwater Aquatic Macrophytes. *Organic Geochemistry*, 31(7–8): 745–749. https://doi.org/10.1016/S0146-6380(00)00081-4

Freeman, K. H., Colarusso, L. A., 2001. Molecular and Isotopic Records of C_4 Grassland Expansion in the Late Miocene. *Geochimica et Cosmochimica Acta*, 65(9): 1439–1454. https://doi.org/10.1016/s0016-7037(00)00573-1

Freeman, K. H., Hayes, J. M., Trendel, J. M., et al., 1990. Evidence from Carbon Isotope Measurements for Diverse Origins Of Sedimentary Hydrocarbons. *Nature*, 343(6255): 254–256. https://doi.org/10.1038/343254a0

Freeman, K. H., Wakeham, S. G., Hayes, J. M., 1994. Predictive Isotopic Biogeochemistry: Hydrocarbons from Anoxic Marine Basins. *Organic Geochemistry*, 21(6–7): 629–644. https://doi.org/10.1016/0146-6380(94)90009-4

Gallego-Torres, D., Martinez-Ruiz, F., Paytan, A., et al., 2007. Pliocene-Holocene Evolution of Depositional Conditions in the Eastern Mediterranean: Role of Anoxia *vs*. Productivity at Time of Sapropel Deposition. *Palaeogeography, Palaeoclimatology, Palaeoecology*, 246(2–4): 424–439. https://doi. org/10.1016/j.palaeo.2006.10.008

González, C. R., 1990. Development of the Late Paleozoic Glaciations of the South American Gondwana in Western Argentina. *Palaeogeography*, *Palaeoclimatology*, *Palaeoecology*, 79(3–4): 275–287. https://doi.org/10.1016/0031-0182(90)90022-y

Gürgey, K., 1999. Geochemical Characteristics and Thermal Maturity of Oils from the Thrace Basin (Western Turkey) and Western Turkmenistan. *Journal of Petroleum Geology*, 22(2): 167–189. https://doi.org/10.1111/j.1747-5457.1999.tb00466.x

Hedges, J. I., Keil, R. G., Benner, R., 1997. What Happens to Terrestrial Organic Matter in the Ocean? *Organic Geochemistry*, 27(5-6): 195–212. https://doi.org/10.1016/s0146-6380(97)00066-1

Holba, A. G., Ellis, L., Dzou, I. L., et al., 2001. Extended Tricyclic Terpanes as Age Discriminators between Triassic, Early Jurassic and Middle–Late Jurassic Oils. In 20th International Meeting on Organic Geochemistry, 1: 464. EAOG Nancy, France

Hollander, D. J., McKenzie, J. A., 1991. CO_2 Control on Carbon-Isotope Fractionation during Aqueous Photosynthesis: A Paleo-pCO_2 Barometer. *Geology*, 19(9): 929–932. https://doi. org/10.1130/0091-7613(1991)019<0929:ccocif>2.3.co;2

Hou, M. G., Zha, M., Ding, X. J., et al., 2021. Source and Accumulation Process of Jurassic Biodegraded Oil in the Eastern Junggar Basin, NW China. *Petroleum Science*, 18(4): 1033–1046. https://doi.org/10.1016/j.petsci.2021.07.010

Huang, B. J., Zhu, W. L., Tian, H., et al., 2017. Characterization of Eocene Lacustrine Source Rocks and Their Oils in the Beibuwan Basin, Offshore South China Sea. *AAPG Bulletin*, 101(9): 1395–1423. https://doi.org/10.1306/10171615161

Huang, W. Y., Meinschein, W. G., 1979. Sterols as Ecological Indicators. *Geochimica et Cosmochimica Acta*, 43(5): 739–745. https://doi.org/10.1016/0016-7037(79)90257-6

Huang, Y. S., Street-Perrott, F. A., Perrott, R. A., et al., 1999. Glacial-Interglacial Environmental Changes Inferred from Molecular and Compound-Specific $\delta^{13}C$ Analyses of Sediments from Sacred Lake, Mt. Kenya. *Geochimica et Cosmochimica Acta*, 63(9): 1383–1404. https://doi.org/10.1016/s0016-7037(99)00074-5

Hunt, J. M., 1979. Petroleum Geochemistry and Geology. Freman, New York, 261–273

Hunt, J. M., 1996. Petroleum Geochemistry and Geology. W. H. Freeman and Company, New York

Jarvie, D. M., 2012. Shale Resource Systems for Oil and Gas: Part 1—Shale-Gas Resource Systems. *American Association of Petroleum Geologists Memoir*, *97:* 69–87. https://doi. org/10.1306/13321446m973489

Kruge, M. A., Hubert, J. F., Bensley, D. F., et al., 1990. Organic Geochemistry of a Lower Jurassic Synrift Lacustrine Sequence, Hartford Basin, Connecticut, USA. *Organic Geochemistry*, 16(4–6): 689–701. https://doi.org/10.1016/0146-6380(90)90110-I

Kuang, L. C., Tang, Y., Lei, D. W., et al., 2012. Formation Conditions and Exploration Potential of Tight Oil in the Permian Saline Lacustrine Dolomitic Rock, Junggar Basin, NW China. *Petroleum Exploration and Development*, 39(6): 700–711. https://doi.org/10.1016/s1876-3804(12)60095-0

Lamb, A. L., Wilson, G. P., Leng, M. J., 2006. A Review of Coastal Palaeoclimate and Relative Sea-Level Reconstructions Using $\delta^{13}C$ and C/N Ratios in Organic Material. *Earth-Science Reviews*, 75(1–4): 29–57. https://doi.org/10.1016/j.earscirev.2005.10.003

Langford, F. F., Blanc-Valleron, M. M., 1990. Interpreting Rock-Eval Pyrolysis Data Using Graphs of Pyrolizable Hydrocarbons vs. Total Organic Carbon (1). *American Association of Petroleum Geologists Bulletin*, 74(6): 799–804. https://doi.org/10.1306/0c9b238f-1710-11d7-8645000102c1865d

Li, M. W., Chen, Z. H., Cao, T. T., et al., 2018. Expelled Oils and Their Impacts On Rock-Eval Data Interpretation, Eocene Qianjiang Formation in Jianghan Basin, China. *International Journal of Coal Geology*, 191: 37–48. https://doi.org/10.1016/j.coal.2018.03.001

Liang, J. L., Tang, D. Z., Xu, H., et al., 2014. Formation Conditions of Jimusaer Oil Shale at the Northern Foot of Bogda Mountain, China. *Oil Shale*, 31(1): 19–29. https://doi.org/10.3176/oil.2014.1.03

Liu, Q. Y., Li, P., Jin, Z. J., et al., 2021. Preservation of Organic Matter in Shale Linked to Bacterial Sulfate Reduction (BSR) and Volcanic Activity under Marine and Lacustrine Depositional Environments. *Marine and Petroleum Geology*, 127: 104950. https://doi.org/10.1016/j.marpetgeo.2021.104950

Luo, Q. Y., George, S. C., Xu, Y. H., et al., 2016. Organic Geochemical Characteristics of the Mesoproterozoic Hongshuizhuang Formation from Northern China: Implications for Thermal Maturity and Biological Sources. *Organic Geochemistry*, 99: 23–37. https://doi.org/10.1016/j.orggeochem.2016.05.004

Luo, Q. Y., Gong, L., Qu, Y. S., et al., 2018. The Tight Oil Potential of the Lucaogou Formation from the Southern Junggar Basin, China. *Fuel*, 234: 858–871. https://doi.org/10.1016/j.fuel.2018.07.002

Mackie, E. A. V., Leng, M. J., Lloyd, J. M., et al., 2005. Bulk Organic $\delta^{13}C$ and C/N Ratios as Palaeosalinity Indicators within a Scottish Isolation Basin. *Journal of Quaternary Science*, 20(4): 303–312. https://doi.org/10.1002/jqs.919

Marynowski, L., Narkiewicz, M., Grelowski, C., 2000. Biomarkers as Environmental Indicators in a Carbonate Complex, Example from the Middle to Upper Devonian, Holy cross Mountains, Poland. *Sedimentary Geology*, 137(3–4): 187–212. https://doi.org/10.1016/s0037-0738(00)00157-3

McLennan, S. M., 2001. Relationships between the Trace Element Composition of Sedimentary Rocks and Upper Continental Crust. *Geochemistry Geophysics Geosystems*, 2(4): 2000GC000109. https://doi.org/10.1029/2000gc000109

Meyers, P. A., 1994. Preservation of Elemental and Isotopic Source Identification of Sedimentary Organic Matter. *Chemical Geology*, 144(3-4): 289-302. https://doi.org/10.1016/0009-2541(94)90059-0

Meyers, P. A., 1997. Organic Geochemical Proxies of Paleoceanographic, Paleolimnologic, and Paleoclimatic Processes. *Organic Geochemistry*, 27(5–6): 213–250. https://doi.org/10.1016/S0146-6380(97)00049-1

Moldowan, J. M., Seifert, W. K., Gallegos, E. J., 1985. Relationship between Petroleum Composition and Depositional Environment of Petroleum Source Rocks. *American Association of Petroleum Geologists Bulletin*, 69(8): 1255–1268. https://doi.org/10.1306/ad462bc8-16f7-11d7-8645000102c1865d

Mort, H., Jacquat, O., Adatte, T., et al., 2007. The Cenomanian/Turonian Anoxic Event at the Bonarelli Level in Italy and Spain: Enhanced Productivity and/or Better Preservation? *Cretaceous Research*, 28(4): 597–612. https://doi.org/10.1016/j.cretres.2006.09.003

Nameroff, T. J., Garant, R. J., Albert, M. B., 2004. Adoption of Green Chemistry: An Analysis Based on US Patents. *Research Policy*, 33(6–7): 959–974. https://doi.org/10.1016/j.respol.2004.03.001

Nichols, J. E., Booth, R. K., Jackson, S. T., et al., 2006. Paleohydrologic Reconstruction Based on *n*-Alkane Distributions in Ombrotrophic Peat. *Organic Geochemistry*, 37(11): 1505–1513. https://doi.org/10.1016/j.orggeochem.2006.06.020

Ourisson, G., Albrecht, P., 1992. Hopanoids. 1. Geohopanoids: The Most Abundant Natural Products on Earth? *Accounts of Chemical Research*, 25(9): 398–402. https://doi.org/10.1021/ar00021a003

Ourisson, G., Rohmer, M., 1992. Hopanoids. 2. Biohopanoids: A Novel Class of Bacterial Lipids. *Accounts of Chemical Research*, 25(9): 403–408. https://doi.org/10.1021/ar00021a004

Peters, K. E., 1986. Guidelines for Evaluating Petroleum Source Rock Using Programmed Pyrolysis. *American Association of Petroleum Geologists Bulletin*, 70(3): 318–329. https://doi.org/10.1306/94885688-1704-11d7-8645000102c1865d

Peters, K. E., Moldowan, J. M., 1991. Effects of Source, Thermal Maturity, and Biodegradation on the Distribution and Isomerization of Homohopanes in Petroleum. *Organic Geochemistry*, 17(1): 47–61. https://doi.org/10.1016/0146-6380(91)90039-m

Peters, K. E., Moldowan, J. M., 1993. The Biomarker Guide. Englewood Cliffs, Prentice Hall, New Jersey. 363

Peters, K. E., Walters, C. C., Moldowan, J. M., 2005. The Biomarker Guide: Column 2, Biomarkers and Isotopes in Petroleum Systems and Earth History. 2nd Edition. Cambridge University Press, Cambridge

Piper, D. Z., Perkins, R. B., 2004. A Modern *vs.* Permian Black Shale—The Hydrography, Primary Productivity, and Water-Column Chemistry of Deposition. *Chemical Geology*, 206 (3–4): 177–197. https://doi.org/10.1016/j.chemgeo.2003.12.006

Qiao, J. Q., Baniasad, A., Zieger, L., et al., 2021a. Paleo-Depositional Environment, Origin and Characteristics of Organic Matter of the Triassic Chang 7 Member of the Yanchang Formation throughout the Mid-Western Part of the Ordos Basin, China. *International Journal of Coal Geology*, 237: 103636. https://doi.org/10.1016/j.coal.2020.103636

Qiao, J. Q., Grohmann, S., Baniasad, A., et al., 2021b. High Microbial Gas Potential of Pleistocene Lacustrine Deposits in the Central Qaidam Basin, China: An Organic Geochemical and

Petrographic Assessment. *International Journal of Coal Geology*, 245: 103818. https://doi.org/10.1016/j.coal.2021.103818

Qiao, J. Q., Littke, R., Grohmann, S., et al., 2022. Climatic and Environmental Conditions during the Pleistocene in the Central Qaidam Basin, NE Tibetan Plateau: Evidence from GDGTs, Stable Isotopes and Major and trace Elements of the Qigequan Formation. *International Journal of Coal Geology*, 254: 103958. https://doi.org/10.1016/j.coal.2022.103958

Qiao, J. Q., Liu, L. F., Shang, X. Q., 2020. Deposition Conditions of the Jurassic Lacustrine Source Rocks in the East Fukang Sag, junggar Basin, NW China: Evidence from Major and Race Elements. *Geological Journal*, 55 (7): 4936–4953. https://doi.org/10.1002/gj.3714

Reed, R. M., Loucks, R. G., Ruppel, S. C., 2014. Comment on "Formation of Nanoporous Pyrobitumen Residues during Maturation of the Barnett Shale (Fort Worth Basin)" by Bernard et al. (2012). *International Journal of Coal Geology*, 127: 111–113. https://doi.org/10.1016/j.coal.2013.11.012

Requejo, A. G., Hieshima, G. B., Hsu, C. S., et al., 1997. Short-Chain (C_{21} and C_{22}) Diasteranes in Petroleum and Source Rocks as Indicators of Maturity and Depositional Environment. *Geochimica et Cosmochimica Acta*, 61(13): 2653–2667. https://doi.org/10.1016/s0016-7037(97)00106-3

Riboulleau, A., Schnyder, J., Riquier, L., et al., 2007. Environmental Change during the Early Cretaceous in the Purbeck-Type Durlston Bay Section (Dorset, Southern England): A Biomarker Approach. *Organic Geochemisty*, 38(11): 1804–1823. https://doi.org/10.1016/j.orggeochem.2007.07.006

Rimmer, S. M., 2004. Geochemical Paleoredox Indicators in Devonian – Mississippian Black Shales, Central Appalachian Basin (USA). *Chemical Geology*, 206(3–4): 373–391. https://doi.org/10.1016/j.chemgeo.2003.12.029

Robinson, S. A., Hesselbo, S. P., 2004. Fossil-Wood Carbon-Isotope Stratigraphy of the Non-Marine Wealden Group (Lower Cretaceous, Southern England). *Journal Geological Society*, 161(1): 133–145. https://doi.org/10.1144/0016-764903-004

Romero-Viana, L., Kienel, U., Sachse, D., 2012. Lipid Biomarker Signatures in a Hypersaline Lake on Isabel Island (Eastern Pacific) as a Proxy for Past Rainfall Anomaly (1942–2006 AD). *Palaeogeography*, *Palaecolimatology*, *Palaeoecology*, 350–352: 49–61. https://doi.org/10.1016/j.palaeo.2012.06.011

Ross, D. J. K., Bustin, R. M., 2009. Investigating the Use of Sedimentary Geochemical Proxies for Paleoenvironment Interpretation of Thermally Mature Organic-Rich Strata: Examples from the Devonian – Mississippian Shales, Western Canadian Sedimentary Basin. *Chemical Geology*, 260(1–2): 1–19. https://doi.org/10.1016/j.chemgeo.2008.10.027

Schoepfer, S. D., Shen, J., Wei, H. Y., et al., 2015. Total Organic Carbon, Organic Phosphorus, and Biogenic Barium Fluxes as Proxies for Paleomarine Productivity. *Earth-Science Reviews*, 149: 23–52. https://doi.org/10.1016/j.earscirev.2014.08.017

Shanmugam, G., 1985. Significance of Coniferous Rain Forests and Related Organic Matter in Generating Commercial Quantities of Oil, Gippsland Basin, Australia 1. *American Association of Petroleum Geologists Bulletin*, 69(8): 1241–1254. https://doi.org/10.1306/ad462bc3-16f7-11d7-8645000102c1865d

Shiea, J., Brassell, S. C., Ward, D. M., 1990. Mid-Chain Branched Mono-and Dimethyl Alkanes in Hot Spring Cyanobacterial Mats: a Direct Biogenic Source for Branched Alkanes in Ancient Sediments?. *Organic Geochemistry*, 15(3): 223–231. https://doi.org/10.1016/0146-6380(90)90001-g

Sinninghe Damsté, J. S., Kenig, F., Koopmans, M. P., et al., 1995. Evidence for Gammacerane as an Indicator of Water Column Stratification. *Geochimica et Cosmochimica Acta*, 59(9): 1895–1900. https://doi.org/10.1016/0016-7037(95)00073-9

Summons, R. E., Powell, T. G., 1987. Identification of Aryl Isoprenoids in Source Rocks and Crude Oils: Biological Markers for the Green Sulphur Bacteria. *Geochimica et Cosmochimica Acta*, 51(3): 557 – 566. https://doi. org/10.1016/0016-7037(87)90069-x

Tan, J. Q., Wang, Z. H., Wang, W. H., et al., 2021. Depositional Environment and Hydrothermal Controls on Organic Matter Enrichment in the Lower Cambrian Niutitang Shale, Southern China. *AAPG Bulletin*, 105(7): 1329 – 1356. https://doi. org/10.1306/12222018196

ten Haven, H. L., de Leeuw, J. W., Rullkötter, J. et al., 1987. Restricted Utility of the Pristane/Phytane Ratio as a Palaeoenvironmental Indicator. *Nature*, 330 (6149): 641 – 643. https://doi.org/10.1038/330641a0

Vaezian, A., Ziaii, M., Kamali, M. R., et al., 2014. An Evaluation on Geochemical Characteristics of Some Probable Source Rocks of Salman Oil Field in the Persian Gulf. *Arabian Journal for Science and Engineering*, 39(7): 5653 – 5663. https://doi. org/10.1007/s13369-014-1129-0

Volk, H., George, S. C., Middleton, H., et al., 2005. Geochemical Comparison of Fluid Inclusion and Present-Day Oil Accumulations in the Papuan Foreland-Evidence for Previously Unrecognised Petroleum Source Rocks. *Organic Geochemistry*, 36(1): 29–51. https://doi.org/10.1016/j.orggeochem.2004.07.018

Volkman, J. K., 2003. Sterols in Microorganisms. *Applied Microbiology and Biotechnology*, 60(5): 495–506. https://doi.org/10.1007/s00253-002-1172-8

Wan, Z. F., Shi, Q. H., Zhang, Q., et al., 2015. Characteristics and Developmental Mechanisms of Mud Volcanoes on the Southern Margin of the Junggar Basin, NW China. *Geological Journal*, 50(4): 434–445. https://doi.org/10.1002/gj.2547

Wang, G. L., Chang, X. C., Wang, T. G., et al., 2015. Pregnanes as Molecular Indicators for Depositional Environments of Sediments and Petroleum Source Rocks. *Organic Geochemistry*, 78: 110–120. https://doi.org/10.1016/j.orggeochem.2014.11.004

Waseda, A., Nishita, H., 1998. Geochemical Characteristics of Terrigenous- and Marine-Sourced Oils in Hokkaido, Japan. *Organic Geochemistry*, 28(1–2): 27–41. https://doi.org/10.1016/s0146-6380(97)00102-2

Wu, Z. R., Grohmann, S., Littke, R., et al., 2022a. Organic Petrologic and Geochemical Characterization of Petroleum Source Rocks in the Middle Jurassic Dameigou Formation, Qaidam Basin, Northwestern China: Insights into Paleo-Depositional Environment and Organic Matter Accumulation. *International Journal of Coal Geology*, 259. https://doi.org/10.1016/j.coal.2022.104038

Wu, Z. R., He, S., He, Z. L., et al., 2022. Petrographical and Geochemical Characterization of the Upper Permian Longtan Formation and Dalong Formation in the Lower Yangtze Region, South China: Implications for Provenance, Paleoclimate, Paleoenvironment and Organic Matter Accumulation

Mechanisms. *Marine and Petroleum Geology*, 139: 105580. https://doi.org/10.1016/j.marpetgeo.2022.105580

Xie, X. M., Borjigin, T., Zhang, Q. Z., et al., 2015. Intact Microbial Fossils in the Permian Lucaogou Formation Oil Shale, Junggar Basin, NW China. *International Journal of Coal Geology*, 146: 166–178. https://doi.org/10.1016/j.coal.2015.05.011

Zhang, Q., Grohmann, S., Xu, X. C., et al., 2020. Depositional Environment and Thermal Maturity of the Coal-Bearing Longtan Shale in Southwest Guizhou, China: Implications for Shale Gas Resource Potential. Intertatiaon *Journal of Coal Geology*, 231: 103607, https://doi.org/10.1016/j.coal.2020.103607

Zhang, Z. J., Cheng, D. W., Zhou, C. M., et al., 2021. Characteristics of Fine-Grained Rocks in the Pingdiquan Formation in Well Shishu 1 and Their Significances for Shale Oil Explorations in Northeastern Junggar Basin. *Natural Gas Geoscience*, 32(4): 562–576 (in Chinese with English Abstract)

Zhao, J. H., Jin, Z. J., Jin, Z. K., et al., 2016. Applying Sedimentary Geochemical Proxies for Paleoenvironment Interpretation of Organic-Rich Shale Deposition in the Sichuan Basin, China. *International Journal of Coal Geology*, 163: 52 – 71. https://doi.org/10.1016/j.coal.2016.06.015

Zheng, T. Y., Zieger, L., Baniasad, A., et al., 2022. The Shahejie Formation in the Dongpu Depression, Bohai Bay Basin, China: Geochemical Investigation of the Origin, Deposition and Preservation of Organic Matter in a Saline Lacustrine Environment during the Middle Eocene. *International Journal of Coal Geology*, 253: 103967. https://doi.org/10.1016/j.coal.2022.103967

Zhu, G. Y., Li, T. T., Zhang, Z. Y., et al., 2022. Nitrogen Isotope Evidence for Oxygenated Upper Ocean during the Cryogenian Interglacial Period. *Chemical Geology*, 604: 120929. https://doi.org/10.1016/j.chemgeo.2022.120929

Zhu, H. C., Ouyang, S., Zhan, J. Z., et al., 2005. Comparison of Permian Palynological Assemblages from the Junggar and Tarim Basins and Their Phytoprovincial Significance. *Review of Palaeobotany Palynology*, 136(3–4): 181–207. https://doi.org/10.1016/j.revpalbo.2005.07.001